Proc. Natl. Acad. Sci. USA
Vol. 94, pp. 1550–1555, February 1997
Neurobiology

Amyloid precursor protein processing and $A\beta_{42}$ deposition in a transgenic mouse model of Alzheimer disease

(PDAPP mouse/β-peptide/amyloidogenesis)

K. JOHNSON-WOOD, M. LEE, R. MOTTER, K. HU, G. GORDON, R. BARBOUR, K. KHAN, M. GORDON, H. TAN, D. GAMES, I. LIEBERBURG, D. SCHENK, P. SEUBERT*, AND L. MCCONLOGUE

Athena Neurosciences, Inc., 800 Gateway Boulevard, South San Francisco, CA 94080

Communicated by L. Iversen, University of Oxford, Oxford, United Kingdom, December 6, 1996 (received for review August 18, 1996)

ABSTRACT **The PDAPP transgenic mouse, which overexpresses human amyloid precursor protein (APP717V→F), has been shown to develop much of the pathology associated with Alzheimer disease. In this report, levels of APP and its amyloidogenic metabolites were measured in brain regions of transgenic mice between 4 and 18 months of age. While absolute levels of APP expression likely contribute to the rate of amyloid β-peptide (Aβ) deposition, regionally specific factors also seem important, as homozygotic mice express APP levels in pathologically unaffected regions in excess of that measured in certain amyloid plaque-prone regions of heterozygotic mice. Regional levels of APP and APP-β were nearly constant at all ages, while Aβ levels dramatically and predictably increased in brain regions undergoing histochemically confirmed amyloidosis, most notably in the cortex and hippocampus. In hippocampus, Aβ concentrations increase 17-fold between the ages of 4 and 8 months, and by 18 months of age are over 500-fold that at 4 months, reaching an average level in excess of 20 nmol of Aβ per g of tissue. $A\beta_{1-42}$ constitutes the vast majority of the depositing Aβ species. The similarities observed between the PDAPP mouse and human Alzheimer disease with regard to $A\beta_{42}$ deposition occurring in a temporally and regionally specific fashion further validate the use of the model in understanding processes related to the disease.**

In the Alzheimer disease (AD) brain, region-specific amyloid β-peptide (Aβ) amyloidosis is a key pathological feature and is accompanied by astrogliosis, microgliosis, cytoskeletal changes, and synaptic loss. These pathological alterations are thought to be linked to the cognitive decline that clinically defines the disease (1). AD primarily afflicts the elderly, although genetic mutations in the amyloid precursor protein (APP) gene have been described that accelerate the disease process and lower the average age of onset by decades, further supporting a fundamental role for this protein in the disease (2–5). Many questions remain about the spatial–temporal sequence of neuropathological events, particularly what factors are responsible for the selective vulnerability of certain brain regions to amyloidosis. Candidate mechanisms include constitutive increased production of Aβ in vulnerable areas, age-related changes in expression of APP and production of Aβ, and inherent differences in the ability of different brain regions to clear or catabolize Aβ. These fundamental issues are not easily addressed in human subjects.

Similar neuropathology to that seen in human AD brain has been demonstrated in a transgenic mouse generated using a platelet-derived growth factor β promoter driving a human APP minigene (6) and possessing the familial AD mutation V→F at APP position 717 (4) (PDAPP). These animals express high levels of APP and Aβ, but more importantly they exhibit profuse Aβ amyloidosis, which, in an age- and brain region-specific manner, morphologically resembles that seen in AD. In addition, these mice develop marked astrogliosis, microgliosis, cytoskeletal changes, and synaptic loss. They offer the opportunity to examine the biological events leading to amyloidosis and synaptic loss and provide an effective animal model to test for therapeutic agents that have the ability to retard or interfere in these pathological processes.

In this report, we quantitatively assess the profile of a number of APP-derived protein species in different brain regions at various ages in these PDAPP transgenic mice. This is addressed through the use of enzyme-linked immunoassays (ELISAs) configured with antibodies specific to Aβ, $A\beta_{1-42}$, APP cleaved at the β-secretase site (7), and APP containing the first 12 aa of Aβ [i.e., α-secretase-cleaved (8) and full-length (FL) APP]. These biochemical measurements were then compared with the regional distribution of amyloid plaques visualized immunohistochemically. The results suggest that age, Aβ production levels, and brain region-specific factors all likely play critical roles in amyloid deposition in the PDAPP mouse. Striking similarities in both the regional distribution and depositing form of Aβ are noted between the mouse model and the human AD condition. Because of the magnitude and temporal predictability of Aβ deposition, the PDAPP mouse is a practical model in which to test agents that either inhibit the processing of APP to Aβ or retard Aβ amyloidosis.

MATERIALS AND METHODS

Transgenic Animals. The founder of PDAPP line 109 was produced on a Swiss Webster × $B_6D_2F_1$ (C57Bl/6 × DBA/2) background (all strains from Taconic Farms) and bred for three generations with animals of the same background. Generation 3 was bred with $B_6D_2F_1$. Generation 4 was bred with Swiss Webster to produce the outbred heterozygous animals used for these experiments, except where noted. Generation 4 heterozygous animals were bred together to obtain a homozygous animal colony. Generation 4 animals were also bred with C57Bl/6 (The Jackson Laboratory) for five generations to produce a line with a more inbred background. Gross effects on longevity have not been observed in the transgenic lines compared with littermate controls.

Brain Tissue Preparation. The heterozygote transgenic (6, 9) and nontransgenic littermate animals were perfused intracardially with ice-cold 0.9% saline. The brain was removed and one hemisphere was prepared for immunohistochemical anal-

The publication costs of this article were defrayed in part by page charge payment. This article must therefore be hereby marked "*advertisement*" in accordance with 18 U.S.C. §1734 solely to indicate this fact.

0027-8424/97/941550-6$2.00/0
PNAS is available online at **http://www.pnas.org**.

Abbreviations: AD, Alzheimer disease; Aβ, amyloid β-peptide; FL, full-length; RT, room temperature.

*To whom reprint requests should be addressed.

ysis, while three brain regions (cerebellum, hippocampus, and cortex) were dissected from the other hemisphere and used for Aβ and APP measurements. For comparative studies of homozygous and heterozygous animals, an additional sample enriched in thalamic matter was dissected.

Tissue for ELISAs was homogenized in 10 volumes of ice-cold guanidine buffer (5.0 M guanidine·HCl/50 mM Tris·Cl, pH 8.0). The homogenates were mixed for 3 to 4 hr at room temperature (RT), then either assayed or stored at −20°C before quantitation of Aβ and APP. Preliminary experiments showed the analytes were stable to this storage condition and that synthetic Aβ peptide (Bachem) could be quantitatively recovered when spiked into littermate control brain tissue homogenates (data not shown).

Aβ Measurements. The brain homogenates were further diluted 1:10 with ice-cold casein buffer (0.25% casein/0.05% sodium azide/20 μg/ml aprotinin/5 mM EDTA, pH 8.0/10 μg/ml leupeptin in PBS) before centrifugation (16,000 × *g* for 20 min at 4°C). The Aβ standards (1–40 or 1–42 aa) were prepared such that the final composition included 0.5 M guanidine in the presence of 0.1% bovine serum albumin (BSA).

The "total" Aβ sandwich ELISA consists of the capture antibody 266, which is specific to amino acids 13–28 of Aβ (10), and the biotinylated reporter antibody 3D6, which is specific to amino acids 1–5 of Aβ. The 3D6 antibody does not recognize secreted APP or APP-FL but detects only Aβ species with amino-terminal aspartic acid. The assay has a lower limit of sensitivity of ≈50 pg/ml (11 pM) and showed no crossreactivity to the endogenous murine Aβ peptide at concentrations up to 1 ng/ml (data not shown).

The configuration of the $A\beta_{1-42}$-specific sandwich ELISA employs the capture antibody mAb 21F12 ($A\beta_{33-42}$). Biotinylated 3D6 is also the reporter antibody in this assay, which has a lower limit of sensitivity of ≈125 pg/ml (28 pM; data not shown). An $A\beta_{x-42}$ sandwich ELISA, using 266 as the capture antibody and biotinylated 21F12 as the reporter antibody, was used on a subset of brain homogenates. The low end sensitivity of this assay is ≈250 pg/ml (56 pM; data not shown).

The 266 and 21F12 mAbs were coated at 10 μg/ml into 96-well immunoassay plates (Costar) overnight at RT. The plates were then aspirated and blocked with 0.25% human serum albumin in PBS buffer for at least 1 hr at RT, then stored dessicated at 4°C until use. The plates were rehydrated with wash buffer (0.05% Tween 20 in tris-buffered saline) before use. The samples and standards were added to the plates and incubated at RT for 1 hr. The plates were washed three or more times with wash buffer between each step of the assay.

The biotinylated 3D6, diluted to 0.5 μg/ml in casein assay buffer (0.25% casein/0.05% Tween 20, pH 7.4, in PBS), was incubated in the wells for 1 hr at RT. Avidin–horseradish peroxidase (Vector Laboratories), diluted 1:4000 in casein assay buffer, was added to the wells for 1 hr at RT. The colorimetric substrate, Slow TMB-ELISA (Pierce), was added and allowed to react for 15 min, after which the enzymatic reaction was stopped with addition of 1 M H_2SO_4. Reaction product was quantified using a Molecular Devices Vmax spectrophotometer measuring the difference in absorbance at 450 nm and 650 nm.

APP ELISAs. Two different APP assays were used (see Fig. 1). The first recognizes APP-α and APP-FL, while the second recognizes APP-β [APP ending at the methionine preceding the Aβ domain (7)]. The capture antibody for both the APP-α/FL and APP-β assays is 8E5 (6). The reporter mAb (2H3) for the APP-α/FL assay was generated against amino acids 1–12 of Aβ. The lower limit of sensitivity for the 8E5/2H3 assay is ≈11 ng/ml (150 pM). For the APP-β assay, the polyclonal antibody 192, specific to the carboxyl terminus of the β-secretase cleavage site of APP (7), was used as the reporter. The lower limit of sensitivity of the 8E5/192 assay is ≈43 ng/ml (600 pM).

For both APP assays, the 8E5 mAb was coated onto 96-well Costar plates as described above for 266. Purified recombinant secreted APP-α (the secreted form of APP 751) and APP596 of the 695 form were the reference standards used for the APP-α/FL and APP-β assays, respectively (8). The 5 M guanidine brain homogenate samples were diluted 1:10 in specimen diluent for a final buffer composition of 0.5 M NaCl, 0.1% Nonidet P-40, and 0.5 M guanidine. The APP standards and samples were added to the plate and incubated for 1.5 hr at RT. Biotinylated reporter antibodies 2H3 and 192 were incubated with samples for 1 hr at RT. Streptavidin–alkaline phosphatase (Boehringer Mannheim), diluted 1:1000 in specimen diluent, was incubated in the wells for 1 hr at RT. The fluorescent substrate 4-methyl-umbellipheryl-phosphate, was added, and the plates were read on a Cytofluor 2350 (Millipore) at 365 nm excitation and 450 nm emission.

mAb Production. The immunogens for 3D6 ($A\beta_{1-5}$), 2H3 ($A\beta_{1-12}$), 2G3 ($A\beta_{33-40}$), 21F12 ($A\beta_{33-42}$), and 12H7 ($A\beta_{33-42}$) were separately conjugated to sheep anti-mouse immunoglobulin (Jackson ImmunoResearch). Mice were immunized and hybridomas were generated by standard methods. The hybridoma supernatants were screened for high-affinity mAbs by RIA as previously described (10).

Antibodies 12H7 and 21F12 were demonstrated to show negligible crossreactivity (<0.4%) with $A\beta_{1-40}$ in either ELISA or competitive RIA. Antibody 2G3 was similarly shown to be nonreactive with $A\beta_{1-42}$.

Immunohistochemistry. The tissue from one brain hemisphere of each mouse was drop-fixed in 4% paraformaldehyde and postfixed for 3 days. The tissue was mounted coronally and 40-μm sections were collected using a vibratome. The sections were stored in antifreeze solution (30% glycerol/30% ethylene glycol in 40 mM NaPO4) at −20°C before immunostaining. Every sixth section, from the posterior cortex through the hippocampus, was incubated with the appropriate biotinylated antibody (either 3D6, 2G3, or 12H7) at 4°C, overnight. The sections were then reacted with the horseradish peroxidase–avidin–biotin complex (Vector Laboratories) and developed using 3,3′-diaminobenzidine (DAB) as the chromagen.

RESULTS

Aβ and APP Assays. Fig. 1 illustrates the recognition sites of antibodies used in the Aβ and APP assays. The APP-α/FL assay recognizes secreted APP including the first 12 aa of Aβ. Since the reporter antibody (2H3) is not specific to the α-clip site, occurring between Aβ amino acids 16 and 17 (8), this assay also recognizes APP-FL. Preliminary experiments using immobilized APP antibodies to the cytoplasmic tail of APP-FL to deplete brain homogenates of APP-FL suggest that ≈30–40% of the APP-α/FL APP is APP-FL (data not shown). Due to the specificity of the polyclonal reporter antibody, the APP-β assay recognizes only the APP clipped immediately amino-terminal to Aβ (7).

Aβ immunoreactivity was characterized by size exclusion chromatography (Superose 12, Pharmacia) of brain homogenates. Comparisons were made of 2-, 4-, and 12-month-old transgenic brain specimens as well as a 12-month-old nontransgenic mouse brain homogenate to which $A\beta_{1-40}$ had been spiked at a level roughly equal to that found in the 12-month-old transgenic mice. The elution profiles of the transgenic brain homogenates were similar in that the peak fractions of Aβ immunoreactivity occurred in the same position, a single broad symmetric peak that was coincident with the immunoreactive peak of spiked $A\beta_{1-40}$. Attempts were then made to immunodeplete the Aβ immunoreactivity using resin-bound antibodies against Aβ (mAb 266 against $A\beta_{13-28}$), the secreted forms of APP (mAb 8E5 against $APP_{444-592}$ of the 695 form),

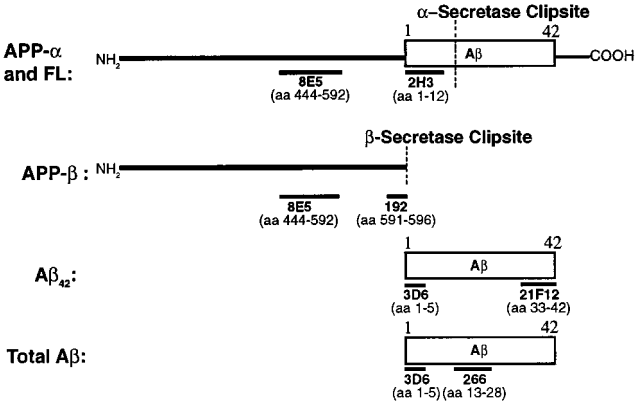

FIG. 1. Immunoassays to forms of Aβ and APP described in the text. Immunoassays were prepared to measure APP-α/FL, APP-β (secreted APP ending at the methionine preceding the start of the Aβ region), and total Aβ. Antibodies are mouse mAbs except 192, which is an affinity-purified rabbit polyclonal antibody. Antibodies 192 and 21F12 are specific to fragments of APP and Aβ, respectively, with carboxyl termini as indicated. Antibody 3D6 is specific for $A\beta_{1-5}$ and does not cross react with APP-α/FL. Methodologies used for the immunoassays are described in text.

the carboxyl terminus of APP (mAb 13G8 $APP_{676-695}$ of the 695 form), or heparin agarose. Only the 266 resin captured Aβ immunoreactivity (data not shown), demonstrating that APP-FL or carboxyl-terminal fragments of APP are not contributing to the Aβ measurement. The $A\beta_{42}$ ELISA uses a capture antibody that recognizes $A\beta_{42}$ but not $A\beta_{1-40}$ peptide. The $A\beta_{42}$ assay, like the total Aβ assay, is not affected by the FL or carboxyl-terminal forms of APP containing Aβ in the homogenates as shown by similar immunodepletion studies (data not shown).

Total Aβ and APP Measurements. Fig. 2 shows the levels of total Aβ, APP-α/FL, and APP-β in the hippocampus, cortex, and cerebellum of transgenic mice as a function of age. Each data point represents the mean value for each age group. The relative levels of APP-α/FL and APP-β in all three brain regions remain relatively constant over time. The hippocampus expresses the highest levels of both APP-α/FL and APP-β followed by the cortex and cerebellum, respectively. The mean ± SD values of all ages for APP-α/FL and APP-β levels in the hippocampus are 720 ± 135 pmol/g and 171 ± 17 pmol/g, respectively. In the hippocampus, the levels of APP-α/FL are approximately 3.5- to 6.0-fold higher than that of APP-β at all ages. Since APP-α/FL is 30–40% APP-FL (see above), we estimate the pool of brain APP to consist of ≈50% APP-α, 30% APP-FL, and 20% APP-β.

Since there was a 1.6-fold increase of APP-α/FL in the hippocampus, which displays robust pathology, versus that of the comparatively unaffected cerebellum, we wanted to determine whether this modest increase of transgenic APP expression was the determinant of the regional pathology displayed in this transgenic line. Western blot analysis of APP transgene expression was performed on brain regions from either heterozygous or homozygous transgenic mice (Fig. 3), both of which show the same regional distribution of pathology (data not shown). There are higher levels of APP expression in the thalamus of the homozygous animal than in the hippocampus of the heterozygous animal; yet pathology in the hippocampus of heterozygotes is extensive with early onset, and the thalamus only displays a minor amount of pathology at later ages. Likewise, there are higher levels of transgene expression in the cerebellum of the homozygous animal, a largely unaffected region, than in the cortex of the heterozygous animal, a region with robust pathology. The same type of comparative analysis was performed on Aβ levels, determined by ELISA, in various brain regions of 2-month-old heterozygous and homozygous transgenic animals (Fig. 3). Although higher levels of Aβ are present in the susceptible brain regions than in unaffected regions in the heterozygotes, the Aβ levels in the thalamus of the homozygotes, which show only minimal pathology in older animals, is equivalent to that in the cortex of the heterozygotes, a region displaying robust pathology at an early age.

In contrast to APP levels, Aβ levels increase dramatically with age in the hippocampus and cortex, with the greatest increase in the hippocampus. No such increase was noted in the cerebellum of the PDAPP transgenic mice (Fig. 2). These region-specific increases of Aβ correlate with the 3D6 immunohistochemical results (Fig. 4 and below). Compared with the levels of 4-month-old mice, Aβ levels increase 8-fold by 8 months of age and 400-fold at 18 months of age in cortex (6330 ± 2310 pmol of Aβ per g of tissue at age 18 months). The corresponding increases in Aβ observed in hippocampus are even more impressive, as the 8-month value is 17 times that at 4 months and increases to 500-fold at 18 months of age (20,800 ± 5250 pmol of Aβ per g of tissue at 18 months).

$A\beta_{42}$ Measurements in Transgenic Mouse Brain. We next determined if, as in human AD subjects (11, 12), the depositing Aβ is the longer $A\beta_{1-42}$ form by measuring the levels of $A\beta_{1-42}$ in the hippocampus and cortex of transgenic mice at different ages. As shown in Table 1, the increase in Aβ observed with age in the hippocampus and cortex of transgenic mice is due

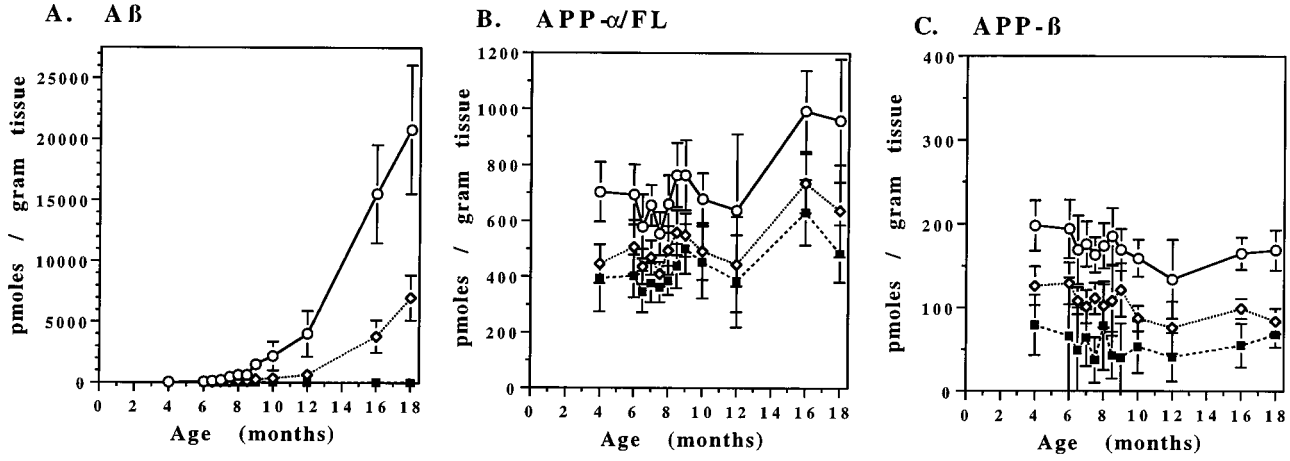

FIG. 2. Age-dependent changes in brain Aβ and APP levels in the PDAPP transgenic mice. PDAPP mice were sacrificed at the ages indicated and levels of Aβ (*A*), APP-β (*B*), and APP-α/FL (*C*) were determined in the cortex (◇), hippocampus (○), and cerebellum (■) by ELISA. Values represent the means ± SD of 9–14 animals.

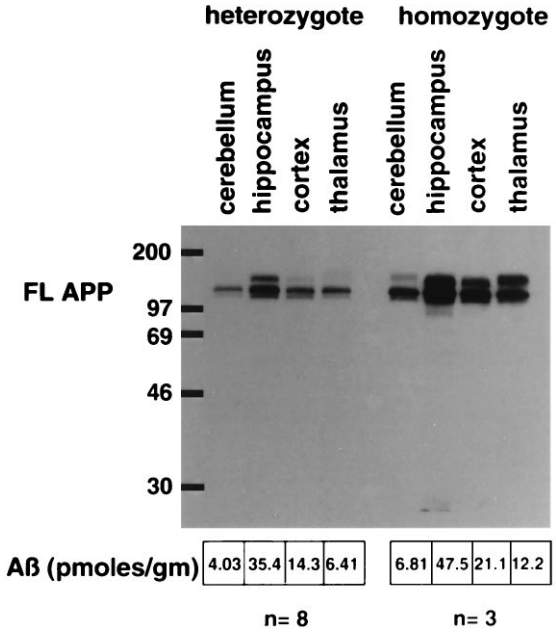

FIG. 3. Levels of APP and Aβ in brain regions of heterozygous and homozygous PDAPP transgenic mice. Two-month-old PDAPP mice were sacrificed, and the amount of APP-FL was measured by Western blot analysis using an APP carboxyl-terminal antibody (anti-6; ref. 6) in hippocampus, cortex, cerebellum, and thalamus of heterozygous and homozygous mice. Essentially similar results were obtained from Western blot analyses using other APP antibodies (human-specific 8E5 and 2H3; data not shown). The amount of Aβ in these same regions from eight heterozygous and three homozygous 2-month-old animals was determined by ELISA, and the average levels are listed.

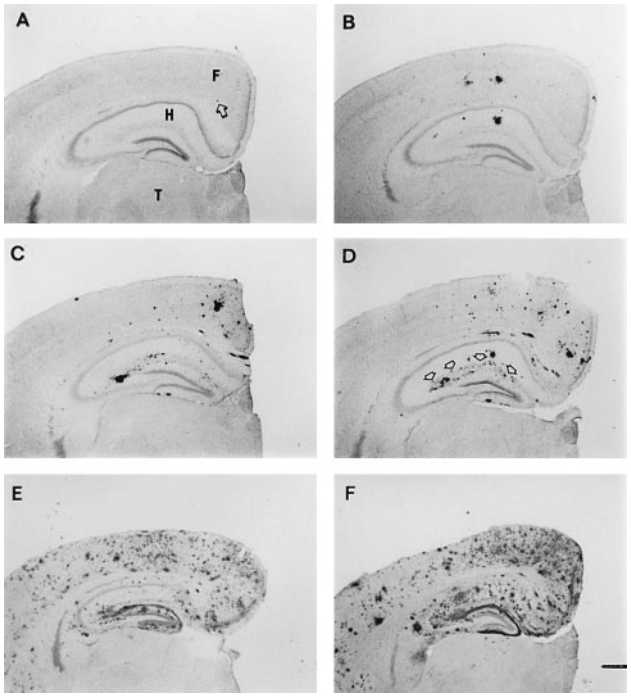

FIG. 4. Age-dependent increases in Aβ plaque burden in the PDAPP mouse. Aβ deposits in the opposite hemisphere of brains used for Aβ and APP ELISAs at 4 (*A*, arrow indicates deposit), 8 (*B*), 10 (*C*), 12 (*D*), 16 (*E*), and 18 (*F*) months of age. Brains are shown from mice with Aβ ELISA values that correspond to the mean of their age group. Deposition typically occurs in an age- and region-dependent manner, with early and heavy involvement of the frontal cortex (F) and hippocampus (H), while the underlying thalamus (T) is devoid of plaques. Arrows in *D* outline the outer molecular layer of the dentate gyrus, which contains terminals from the perforant pathway. [Bar (in *F*) = 500 μm.]

to Aβ_{1-42}. Aβ_{1-42} constituted 27% of the 17 pmol/g of the Aβ present in the brains of young animals, this percentage increased to 89% of the 694 pmol/g in 12-month-old animals. Since the Aβ_{1-42}-specific assay does not detect Aβ_{42} with a truncated or modified amino terminus, further analysis of the Aβ_{42} species in the transgenic mice was performed. A subset (n = 4) of 12-month-old PDAPP transgenic mice cortical homogenates were quantitated in the sandwich ELISA measuring Aβ_{x-42} as well as the Aβ_{1-42}-specific assay. Approximately 90% of the Aβ_{42} is true Aβ_{1-42} and the remaining 10% begins somewhere other than the amino-terminal aspartic acid of Aβ.

Aβ Measurements in Outbred and Inbred Strains of PDAPP Transgenic Mice. The levels of total Aβ in the hippocampus and cortex were compared between the outbred (n = 14) and inbred strains (n = 20) of PDAPP mice at 4 months of age and found to be 15.95 ± 2.70 and 15.51 ± 1.72 pmol/g of tissue in the cortical homogenates and 38.08 ± 6.76 and 33.02 ± 4.56 pmol/g of tissue in the hippocampal homogenates, respectively. Statistical analysis of the cortical and hippocampal Aβ measurements determined that there was not a significant difference in the interanimal variability between the two groups (data not shown).

Aβ Immunohistochemistry in PDAPP Transgenic Brain. To correlate Aβ accumulation in brain as measured by ELISA with the deposition of Aβ into plaques as measured immunohistochemically, opposite hemispheres were sectioned and immunoreacted with 3D6. Fig. 4 illustrates the progression of Aβ deposition in 4-, 8-, 10-, 12-, 16-, and 18-month-old animals, with Aβ measurements representative of the mean value of their age group. At 4 months of age, transgenic brains contain small, rare, punctate deposits, ≈20 μm in diameter, that were only infrequently observed in the hippocampus as well as the frontal and cingulate cortex. By 8 months of age, these regions contain a number of thioflavin-positive Aβ aggregates (data not shown) that form plaques as large as 150 μm in diameter. At 10 months of age, many large Aβ deposits are found throughout the frontal and cingulate cortex and the molecular layers of the hippocampus. The outer molecular layer of the dentate gyrus receiving perforant pathway afferents from the entorhinal cortex is clearly heavily delineated by Aβ deposition. This general pattern was more pronounced by heavier Aβ deposition at 1 year of age, and by 18 months of age it involves most of the neocortex. Notably, a striking increase in Aβ plaque burden paralleled the rising Aβ levels (compare Figs. 2*A* and 4). Staining of sections with antibodies specific for Aβ_{42} (Fig. 5*A*) and Aβ_{40} (Fig. 5*B*) indicates that amyloid plaques are primarily composed of Aβ_{42}, again paralleling the ELISA results. These findings strongly argue that the rise in brain Aβ_{42} concentration determined by ELISA is due to the age-dependent amyloidosis.

Table 1. Aß levels in the cortex of transgenic brain (pmol of Aß per g of wet tissue)

Age, months	n	Aß$_{1-42}$	Total Aß	% Aß$_{42}$
4	11	4.7 ± 1.3	17 ± 3.4	27
8	13	76 ± 40	112 ± 64	68
10	5	247 ± 133	248 ± 139	99
12	9	615 ± 333	694 ± 403	89
16	10	3538 ± 1104	3813 ± 1327	93
18	10	5612 ± 1583	6332 ± 2310	89

Values are in mean ± SD.

DISCUSSION

Aβ amyloidosis is an established diagnostic criteria of AD (13, 14) and is consistently seen in higher-order cortical areas as well as the hippocampal formation of the brain in affected subjects. It is believed that Aβ amyloidosis is a relatively early event in the pathogenesis of AD that subsequently leads to neuronal dysfunction and dementia through a complex cascade of events (15, 16). For unknown reasons, other brain regions, such as the cerebellum, are typically spared from advanced forms of amyloidosis in AD. Both the sequence of events of this process as well as the brain region specificity of AD pathology have been extraordinarily difficult to unravel because brain tissue cannot typically be analyzed until after the death of these patients. Recently, reliable and robust Aβ amyloidosis accompanied by neuropathology has been demonstrated in the PDAPP mouse (6), providing a model in which to study these issues. In this report we have investigated the key metabolites of APP as a function of age and anatomical location and compared this to the immunohistochemically detected changes of Aβ in these animals.

Various pathways of APP processing have been described, including the α-secretase pathway in which cleavage of APP occurs within Aβ (Fig. 1 and ref. 8) and the amyloidogenic or β-secretase pathway in which cleavage of APP occurs at the amino terminus of Aβ (Fig. 1 and ref. 7). Further cleavage of APP leads to the constitutive production of Aβ, including the form ending at position 42 ($A\beta_{42}$). We have taken advantage of site-specific antibodies to develop ELISAs that detect specific APP products arising from these individual pathways in the PDAPP mouse brain.

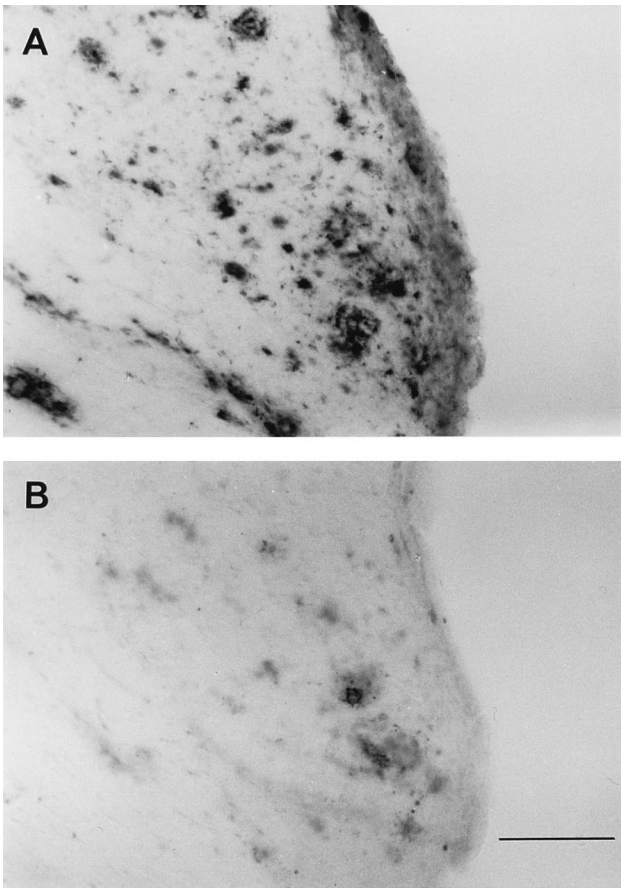

FIG. 5. $A\beta_{42}$ and $A\beta_{40}$ immunohistochemical analysis in 18-month-old PDAPP mice. Aβ deposits in adjacent sections from an 18-month-old mouse visualized with antibodies specific for $A\beta_{42}$ (*A*) and $A\beta_{40}$ (*B*). [Bar (in *B*) = 100 μm.]

Analysis of Aβ and APP immunoreactivities in the PDAPP mouse brain leads to several interesting conclusions. First, levels of APP-α/FL were relatively constant over the age of the PDAPP mice examined and varied only modestly (1.6-fold) among the brain regions analyzed (Fig. 2), indicating that age- or region-dependent changes in expression of the transgene are not amyloidogenic factors in this animal. The lack of amyloid deposition and pathology in the unaffected brain regions in the presence of high levels of APP expression strongly argues that APP overexpression alone is insufficient to cause amyloid deposition in this model. An additional finding that supports this observation is that mice homozygotic for the PDAPP minigene have thalamic levels of APP that exceed those seen in the hippocampus of the heterozygote animals and yet still do not display Aβ deposition in this region (Fig. 3).

To test if region- or age-dependent differential processing of APP to Aβ contributes to Aβ deposition in the PDAPP mouse, we measured the β-secretase product of APP-FL (APP-β) at various ages in different brain regions (7). APP-β is a direct product of β-secretase activity, and its production parallels the production of Aβ *in vitro* under conditions that are expected to either directly modulate the activity of β-secretase or to modulate the accessibility of APP to β-secretase (17–19). Levels of APP-β are therefore thought to correlate with the production of Aβ. The PDAPP mouse thus affords the unique opportunity to measure levels of this metabolite in a tissue destined to undergo amyloidosis at different stages of deposition. Examination of APP-β levels in different brain regions of the PDAPP mouse shows that levels of this APP metabolite do not change significantly with age (Fig. 2). This is true even in the hippocampus where very significant Aβ levels and deposition occur at 8 months of age or greater (Figs. 2 and 4). This finding argues strongly that the age-related amyloid deposition seen in the PDAPP mice is not due to age-dependent increased processing of APP to Aβ mediated by the β-secretory pathway.

Vulnerable brain regions do seem to intrinsically process more APP to Aβ, however. The initial Aβ levels in brains of young animals, before amyloidotic deposition, are higher in hippocampus and cortex than in cerebellum (38.1 pmol/g Aβ in hippocampus, 4.1 pmol/g Aβ in the cerebellum). Levels of APP-β are also higher in amyloid-depositing brain regions; they are 3-fold higher in hippocampus and 2-fold higher in cortex relative to the unaffected cerebellum (Fig. 2). Even normalizing for the 1.5-fold difference in transgenic APP expression between these brain regions, there is 2-fold more APP-β and 7-fold more Aβ in the hippocampus compared with cerebellum, supporting the notion that there is more efficient processing of APP to Aβ in affected brain regions than in unaffected regions. Modest changes in Aβ production, such as in Down syndrome, are sufficient to accelerate amyloid deposition (15). Taken together, these data suggest that increased constitutive processing to Aβ, via the β-secretase pathway, is a significant factor in the brain region specific deposition of Aβ that is seen in the PDAPP mouse.

However, there must be other significant factors in addition to enhanced Aβ production that lead to amyloidosis, since measurements of Aβ or APP-β levels in unaffected brain regions of mice homozygotic for the PDAPP minigene are essentially equivalent to those seen in affected brain regions of the heterozygote PDAPP mice (Fig. 3). This clearly indicates that not only is reaching a threshold level of Aβ required to cause amyloid deposition, but that other regional specific factors are required to interact with Aβ to elicit amyloid deposition. One can only speculate that such factors might include age-dependent expression of specific proteoglycans (20) or specific receptors and binding substances for Aβ such as C1q, Apo E, or APO J (21–23). Such factors may interact with the Aβ peptide and result in its increased aggregation or

fibril formation. The defined regional and time course of amyloid deposition events in this model allow a means to define these factors.

Initial brain levels of Aβ show interanimal variability up to 2-fold. There are no outlying animals with excessively high or absent Aβ. Since the genetic strain of mice can have an effect on transgene phenotype and this line was derived in a highly outbred background, we tested whether the variability could be reduced by crossing it onto an inbred strain. Variability among animals of initial brain Aβ levels does not seem to be due to the genetic variability of the outbred strain since inbred animals displayed the same variability in Aβ as the outbred animals.

Aβ amyloid deposition seen in the PDAPP mouse brain is highly age- and region-specific (Figs. 2 and 4). Amyloid deposition accelerates at around 7 months of age, and by 12 months of age, amyloid deposition is pronounced throughout the hippocampus and in the frontal region of the cortex. Between 12 and 16 months of age, a further dramatic increase in deposition is observed. This anatomical localization of Aβ deposition is remarkably similar to that seen in AD (13). The age-dependent increases in immunohistochemically detectable amyloid deposition correlate well with the dramatic rise in Aβ levels in these brain regions as measured by ELISA. An increase in Aβ is measurable by 7 months of age and by 10 months the hippocampus has 2180 pmol Aβ/g of tissue. By 18 months of age, the levels of $A\beta_{42}$ are comparable to the higher Aβ levels observed in humans with AD (24). Aβ levels in the cerebellum at 10 months, an unaffected brain region, remain at 4 pmol/g of tissue—essentially unchanged relative to the levels at 4 months of age, in agreement with the extent of amyloid deposition observed by histological analyses. Thus, a reproducible increase in measurable Aβ occurs in the brain tissue of the PDAPP mice that correlates with the severity of amyloid deposition. These results suggest that in aged PDAPP mice, monitoring of brain Aβ levels reflects amyloid burden and therefore direct immunoassay measurement of brain Aβ levels can be used to monitor the effects of compounds that reduce amyloid plaque burden.

The vast majority of depositing Aβ in these mice is of the longer $A\beta_{42}$ form, despite the fact that the majority of Aβ produced in younger animals are shorter species (Table 1). The ELISA data suggest that $A\beta_{42}$ is preferentially depositing in the transgenic mice, a result confirmed by immunostaining (Fig. 5). This is in agreement with studies of human AD and of Down syndrome brains, wherein the predominant and initially depositing Aβ is the longer form (11). In this respect, this mouse model again faithfully reproduces human AD pathology, indicating that the biological mechanisms leading to the preferential deposition of $A\beta_{42}$ in AD are conserved in the mouse. At 18 months of age, the percentage of shorter Aβ is essentially the same as at 12 months in both the cortex and hippocampus. Immunohistochemistry suggests that deposition of the $A\beta_{40}$ species is primarily in compacted plaques, as opposed to increasing amyloid angiopathy. The fact that the majority of Aβ detected in the mouse begins at Asp-1 is different from that reported in human AD (24). However, it is not clear how much of the amino-terminal modification in the human occurs after deposition. In AD, the plaques presumably have a residence time of several years, in contrast to several months, as in the case of the PDAPP mouse. The $A\beta_{42}$ found in the cerebrospinal fluid of AD patients is primarily $A\beta_{1-42}$ (unpublished data), suggesting the predominant cleavage sites are not shifted in the mouse from that in AD.

Aside from the insights into Aβ amyloidosis offered by the PDAPP model, there is a practical use of these studies as well. Using these measurements, it is now feasible to test agents that reduce Aβ peptide burden by preventing its production. Compounds designed to prevent or reverse Aβ deposition can also be evaluated in a reasonable *in vivo* fashion. Such agents, designed to prevent or reduce amyloidosis and plaque burden, will afford a new approach to the treatment of AD.

1. Selkoe, D. (1994) *Annu. Rev. Neurosci.* **17,** 489–517.
2. Goate, A., Chartier-Harlin, M.-C., Mullan, M., Brown, J., Crawford, F., *et al.* (1991) *Nature (London)* **349,** 704–706.
3. Chartier-Harlin, M.-C., Crawford, F., Houlden, H., Warren, A., Hughes, D., Fidani, L., Goate, A., Rossor, M., Roques, P., Hardy, J. & Mullan, M. (1991) *Nature (London)* **353,** 844–846.
4. Murrell, J., Farlow, M., Ghetti, B. & Benson, M. (1991) *Science* **254,** 97–99.
5. Mullan, M., Crawford, F., Axelman, K., Houlden, H., Lilies, L., Winblad, B. & Lannfelt, L. (1992) *Nat. Genet.* **1,** 345–347.
6. Games, D., Adams, D., Alessandrini, R., Barbour, R., Berthelette, P., *et al.* (1995) *Nature (London)* **373,** 523–527.
7. Seubert, P., Oltersdorf, T., Lee, M., Barbour, R., Blomquist, C., Davis, D., Bryant, K., Fritz, L., Galasko, D., Thal, L., Lieberburg, I. & Schenk, D. (1993) *Nature (London)* **361,** 260–263.
8. Esch, F., Keim, P., Beattie, E., Blacher, R., Culwell, A., Oltersdorf, T., McClure, D. & Ward, P. (1990) *Science* **248,** 1122–1124.
9. Rockenstein, E., McConlogue, L., Tan, H., Power, M., Masliah, E. & Mucke, L. (1995) *J. Biol. Chem.* **270,** 28257–28267.
10. Seubert, P., Vigo-Pelfrey, C., Esch, F., Lee, M., Dovey, H., Davis, D., Sinha, S., Schlossmacher, M., Whaley, J., Swindlehurst, C., McCormack, R., Wolfert, R., Selkoe, D., Lieberburg, I. & Schenk, D. (1992) *Nature (London)* **359,** 325–327.
11. Iwatsubo, T., Odaka, A., Suzuki, N., Mizusawa, H., Nukina, N. & Ihara, Y. (1994) *Neuron* **13,** 45–53.
12. Roher, A., Lowenson, J., Clarke, S., Wolkow, C., Wang, R., Cotter, R., Reardon, I., Zurcher-Neely, H., Heinrikson, R., Ball, M. & Greenberg, B. (1993) *J. Biol. Chem.* **268,** 3072–3083.
13. Mirra, S., Heyman, A., McKeel, D., Sumi, S., Crain, B., Brownlee, L., Vogel, F., Hughes, J., van Belle, G., Berg, L. & participating Consortium to Establish a Registry for Alzheimer's Disease (CERAD) neuropathologists (1991) *Neurology* **41,** 479–486.
14. Khachaturian, Z. (1985) *Arch. Neurol. (Chicago)* **42,** 1097–1105.
15. Mann, D., Yuonis, N., Jones, D. & Stoddart, R. W. (1992) *Neurodegeneration* **1,** 201–215.
16. Morris, J., Storandt, M., McKeel, D., Rubin, E., Price, J., Grant, E. & Berg, L. (1996) *Neurology* **46,** 707–719.
17. Citron, M., Oltersdorf, T., Haass, C., McConlogue, L., Hung, A., Seubert, P., Vigo-Pelfrey, C., Lieberburg, I. & Selkoe, D. (1992) *Nature (London)* **360,** 672–674.
18. Cai, X.-D., Golde, T. & Younkin, S. (1993) *Science* **259,** 514–516.
19. Knops, J., Suomensaari, S., Lee, M., McConlogue, L., Seubert, P. & Sinha, S. (1995) *J. Biol. Chem.* **270,** 2419–2422.
20. Snow, A., Sekiguchi, R., Nochlin, D., Fraser, P., Kimata, K., Mizutani, A., Arai, M., Schreier, W. & Morgan, D. (1994) *Neuron* **12,** 219–234.
21. Rogers, J., Cooper, N., Webster, S., Schultz, J., McGeer, P., Styren, S., Civin, W., Brachova, L., Bradt, B., Ward, P. & Lieberburg, I. (1992) *Proc. Natl. Acad. Sci. USA* **89,** 10016–10020.
22. Strittmatter, W., Saunders, A., Schmechel, D., Pericak-Vance, M., Enghild, J., Salvesen, G. & Roses, A. (1993) *Proc. Natl. Acad. Sci. USA* **90,** 1977–1981.
23. Ghiso, J., Matsubara, E., Koudinov, A., Choi-Miura, N., Tomita, M., Wisniewski, T. & Frangione, B. (1993) *Biochem. J.* **293,** 27–30.
24. Gravina, S., Ho, L., Eckman, C., Long, K., Otvos, L., Younkin, L., Suzuki, N. & Younkin, S. (1995) *J. Biol. Chem.* **270,** 7013–7016.